Supplementary Materials :

Connecting complex and simplified models of tipping elements: a nonlinear two-forcing emulator for the Atlantic meridional overturning circulation

Amaury Laridon[1], Victor Couplet[2], Justin Gérard[2], Wim Thiery[1], Michel Crucifix[2]

[1]Vrije Universiteit Brussel, Department of Water and Climate, bclimate Research Group, Brussels, Belgium.
[2]UCLouvain, Earth and Life Institute, Louvain-La-Neuve, Belgium.
Corresponding author : Amaury.Laridon@vub.be

S1. GIS Calibration

In this section, we illustrate the calculations in the case where one would also wish to calibrate the GIS by modelling it with a double-fold dynamics involving two forcing variables. For illustration purposes, we assume that the two main forcings driving the evolution of the GIS volume are the global mean atmospheric temperature and the AMOC intensity. Beyond the physical relevance, this choice is interesting because it would allow for a coupled emulator of the AMOC and the GIS as tipping elements. Thus, we assume the following form to model the GIS while accounting for the stabilizing effect of a weakened AMOC.

$$\frac{dV}{dt} = \left(-V^3 + a_2V^2 + b_2V + c_2 + d_2T + e_{21}(1-\Psi)\right)\mu_V(V). \tag{a}$$

For the GIS, we must calibrate the coefficients a_2, b_2, c_2, d_2, and e_{21}. In this case, the same operational assumptions described for the application of the calibration module to the AMOC are applicable. Specifically, two calibration experiments are required: one providing the evolution of the GIS volume over time under forcing exclusively by the temperature anomaly while keeping the AMOC intensity fixed, and another under the opposite condition, where the GIS volume evolves with forcing exclusively by the AMOC intensity. In other words, it is necessary to have a complex model of the GIS capable of producing both of these experiments. In this context, the coordinates of the bifurcation points are denoted as,

$$\{V^+, T_V^+, \Psi_V^+, V^-, T_V^-, \Psi_V^-\}. \tag{b}$$

We denote $EXPC$ as the first calibration experiment of the GIS volume with respect to the global mean temperature anomaly. In this initial sensitivity experiment, the forcing from AMOC intensity is held constant at an arbitrary value, denoted $\Psi_V = \Psi_V^C$. In this case, Eq.(2) is written as,

$$\frac{dV}{dt} = (-V^3 + a_2V^2 + b_2V + c_2 + e_{21}(1-\Psi^C) + d_2T)\mu_V(V). \tag{c}$$

This first sensitivity experiment provides us with the data for the following bifurcation points,

$$\{(V^+, T_V^+), (V^-, T_V^-)\}. \tag{d}$$

In this case with a single forcing variable, the method of Martinez-Monteiro et al.(47) yields,

$$a_2 = \frac{3(V^- + V^+)}{2}, \tag{e}$$

$$b_2 = -3V^-V^+, \tag{f}$$

$$c_2 + e_{21}(1 - \Psi^C) = \frac{T_V^+ V^{-^2}(V^- - 3V^+) - T_V^- V^{+^2}(V^+ - 3V^-)}{2(T_V^- - T_V^+)}, \quad \text{(g)}$$

$$d_2 = -\frac{(V^+ - V^-)^3}{2(T_V^+ - T_V^-)}. \quad \text{(h)}$$

Finally, we refer to $EXPD$ as the second sensitivity experiment in which we fix the global mean temperature $T_V = T_V^D$ at an arbitrary value but vary the intensity of the AMOC Ψ_V. This sensitivity experiment provides us with the coordinates of the following bifurcation points,

$$\{(V^+, \Psi_V^+), (V^-, \Psi_V^-)\} \quad \text{(i)}$$

while equation Eq.(2) takes the following form:

$$\frac{dV}{dt} = \left(-V^3 + a_2 V^2 + b_2 V + c_2 + d_2 T^D + e_{21}(1 - \Psi)\right)\mu_V(V). \quad \text{(j)}$$

We cannot apply exactly the same calculation procedures for the coefficients due to the formulation of the AMOC forcing, which has a different form than those encountered before. We need to slightly adjust the calculation for the coefficients $c_2 + d_2 T^D, e_{21}$ although the methodology to find them remains the same as above. Therefore, we obtain:

$$c_2 + d_2 T^D = V^{+^3} - a_2 V^{+^2} - b_2 V^{\pm} e_{21}(1 - \Psi_V^+), \quad \text{(k)}$$

$$e_{21} = -\frac{(V^+ - V^-)^3}{2(\Psi_V^- - \Psi_V^+)}. \quad \text{(l)}$$

An example of an application exploring the potential effects of cascading and coupling between the AMOC and the GIS can be found in the MSc Thesis of A. Laridon (52), in which such simulations are performed and analysed. However, in that work, the GIS was not calibrated using a complex model of its dynamics; instead, parameter values from the literature (Armstrong McKay et al. (2022)) were used to calibrate the GIS emulator, which nevertheless included both forcing variables. The aim of the MSc Thesis was to demonstrate the relevance of this emulator-based approach, using two forcing variables, for studying the joint evolution of the AMOC and the GIS under realistic emission scenarios.

S2. Parameterization of the AMOC with Three Forcing Variables

We present an example of a generalization of the ATCM in the case where a third forcing variable is added to the AMOC. Physically, it is interesting to separate the freshwater flux forcing into two components: F_{GIS}, associated with the melting of the GIS, and F_O, which represents any other changes in freshwater fluxes. For instance, F_O could be interpreted as the effect of continental glacier melt. In this context, Laridon (52) developed the following parameterization, labelled $ParamB$, for the AMOC model.

$$\frac{d\Psi}{dt} = (-\Psi^3 + a_1 \Psi^2 + b_1 \Psi + c_1 + d_1 T + e_{12} F_{GIS}(V) + f F_O)\mu_\Psi(\Psi). \quad \text{(m)}$$

To apply the ATCM calibration module, an additional calibration experiment using a complex model is required. This experiment aims to perturb the AMOC by introducing a freshwater flux representing variability in glacier melt, while keeping the freshwater flux from GIS melting and the temperature anomaly constant. In this example with the AMOC, the operational framework becomes more challenging to implement; however, we can still easily derive the values of the calibration parameters, including the new parameter f. One observes the inherent limitation of generalizing to more forcing variables in this calibration method, namely that the independent parameter c_1 will now be determined by three factors rather than two. This introduces a new source of error, and the trade-off in the value at which c_1 should be calibrated will involve balancing three dynamics, rather than just two. Further details, as well as the calculated values of the coefficients, can be found in Laridon (52) and in the

notebook *SURFER_pre3.0_ATCM.ipynb.*

S3. Supplementary Figures

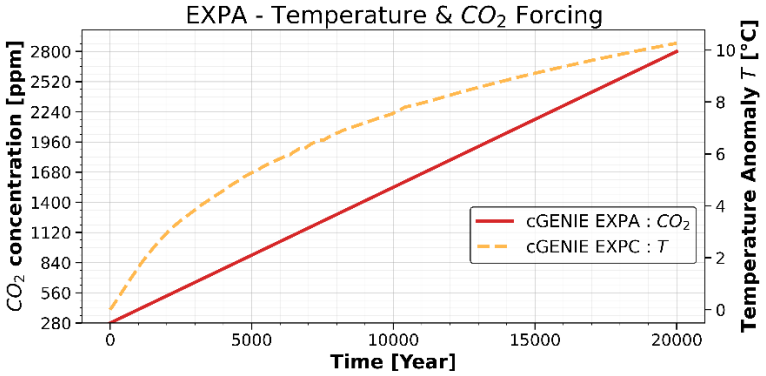

Supplementary Figure 1 | Temperature forcing in the calibration experiment *EXPA* within cGENIE. *EXPA*, consist of a 20,000-year simulation with a prescribed CO_2 forcing increasing linearly from 280 ppm to 2,800 ppm. Through the internal dynamics of cGENIE, this forcing translated into a global mean 2-meter surface air temperature anomaly, starting from $T = 0$ °C and reaching $T = 10$ °C after 20,000 years.

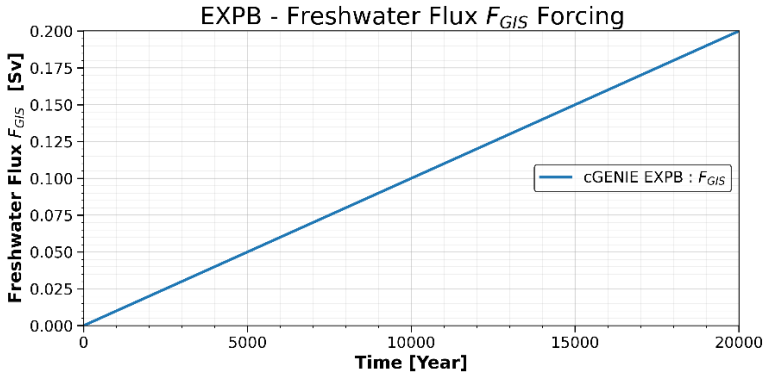

Supplementary Figure 2 | Hosing forcing in the calibration experiment *EXPB* within cGENIE. *EXPB* involved a 20,000 year hosing simulation with freshwater flux forcing ranging from 0 Sv to 0.2 Sv, which is sufficient to induce the collapse of the AMOC in cGENIE. The duration of *EXPB* was chosen to ensure that the AMOC is forced sufficiently slowly, allowing it to remain in equilibrium and produce an hysteresis experiment.

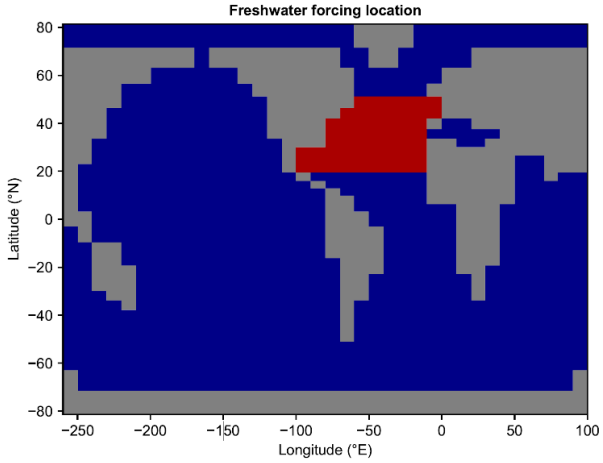

Supplementary Figure 3 | Hosing region in the calibration experiment *EXPB* within cGENIE. The freshwater hosing was applied between 20°N and 50°N across the entire width of the Atlantic.

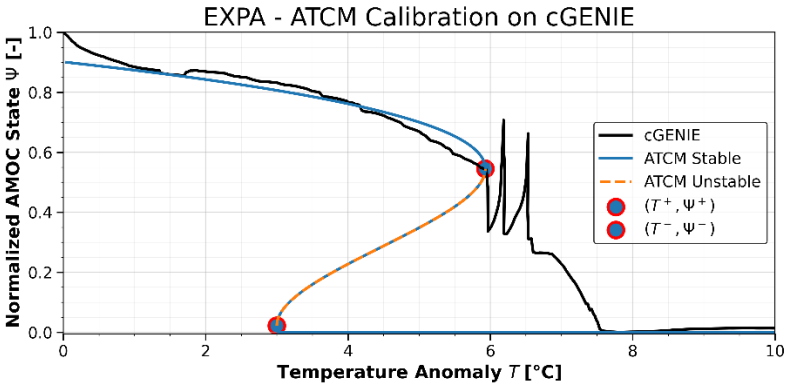

Supplementary Figure 4 | Bifurcation diagram of the AMOC in the calibration experiment *EXPA*. The black curve shows the AMOC trajectory simulated by cGENIE, while the blue curve represents the stable branches obtained from the ATCM. The dashed orange curve highlights the unstable equilibria computed by the ATCM, and the dots indicate the coordinates of the bifurcation points: the upper one identified from cGENIE, and the lower one partially adjusted to improve the fit of the collapse branch.

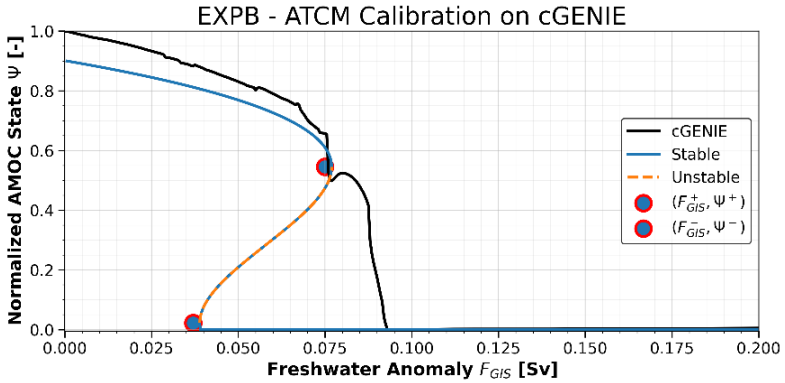

Supplementary Figure 5 | Bifurcation diagram of the AMOC in the calibration experiment *EXPB*. The black curve shows the AMOC trajectory simulated by cGENIE, while the blue curve represents the stable branches obtained from the ATCM. The dashed orange curve highlights the unstable equilibria computed by the ATCM, and the dots indicate the coordinates of the bifurcation points: the upper one identified from cGENIE, and the lower one partially adjusted to improve the fit of the collapse branch.

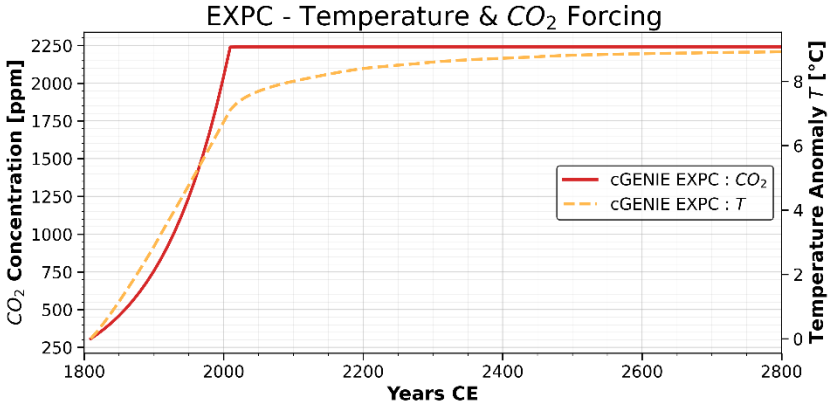

Supplementary Figure 6 | Temperature forcing in the calibration experiment *EXPC* within cGENIE. *EXPC*, consist of a 1,250-year simulation with a prescribed CO_2 atmospheric concentration that increases by 1% a year, starting from 280 ppm and stabilizing at 2240 ppm (i.e., eight times the initial concentration). This forcing, trough the internal dynamics of cGENIE, resulted in a global mean 2-meter surface air temperature anomaly increasing from $T = 0$ °C and reaching $T = 9.07$ °C after 1,250 years.

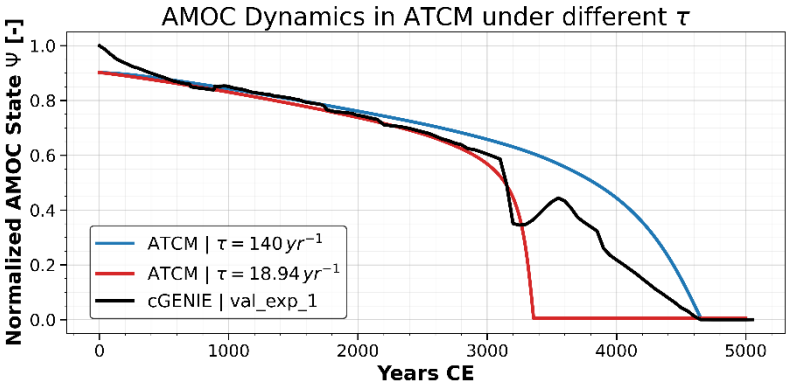

Supplementary Figure 7 | AMOC trajectory in the ATCM under slow forcing with different values of the parameter τ. The black curve shows the AMOC trajectory simulated by cGENIE in the experiment *val_exp_1*, which combines both temperature and freshwater forcing over a long timescale of 20,000 years. In this experiment, atmospheric CO_2 is increased from 280 ppm to 2800 ppm, while the freshwater flux is increased from 0 Sv to 0.2 Sv. The blue curve shows the trajectory simulated by the ATCM when *val_exp_1* is used as the calibration experiment, yielding a parameter value of $\tau = 140\,yr^{-1}$. The red curve shows the emulator trajectory using the value of $\tau = 18.94\,yr^{-1}$ obtained in the main manuscript from the 1% CO_2 increase experiment as $EXPC$.

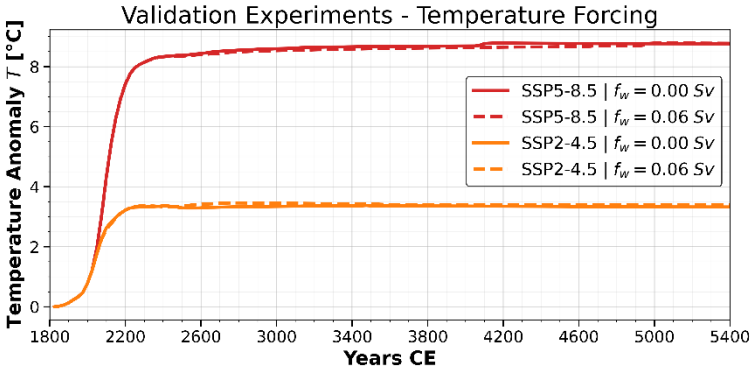

Supplementary Figure 8 | Temperature forcing in the validation experiments within cGENIE. These four simulations follow the atmospheric CO_2 concentrations prescribed by SSP2-4.5 and SSP5-8.5, either without additional freshwater hosing (solid lines) or with hosing (dashed lines). The hosing consists of a constant 0.06 Sv applied throughout the entire simulation, in the same region as previously, namely between 20° N and 50° N across the full width of the Atlantic.